

# Supplementary for Multi-Objective Evolutionary Neural Architecture Search for Liquid State Machine

Sida Xin<sup>1</sup>, Renzhi Chen<sup>2</sup>, Xun Xiao<sup>3</sup>, Yuan Li<sup>3</sup>, Lei Wang<sup>1✉</sup>

## I. PRELIMINARIES

### A. Multi-objective ENAS

Neural architecture search based on multi-objective evolutionary algorithms aims to optimize multiple performance metrics of network architectures simultaneously, such as accuracy and network scale. By simulating the process of natural selection for iterative evolution, this method generates various network architecture candidates, evaluates and selects them based on predetermined multi-objective optimization criteria. Generally, there exists a trade-off between these objectives, meaning that improving one objective may lead to a decrease in performance for another objective. Therefore, the purpose of multi-objective optimization is to find a set of solutions that are considered optimal when all objectives are taken into account. This set of solutions is known as the Pareto optimal set, and the boundary formed by these solutions in the objective space is called the Pareto front [1]. No other solutions can dominate the solutions on the Pareto front. The concept of domination is explained as follows, for any two solutions  $a$  and  $b$ , solution  $a$  dominates solution  $b$  under the following conditions.

$$\forall i, f_i(a) \leq f_i(b) \wedge \exists j, f_j(a) < f_j(b) \quad (1)$$

$f_i(\cdot)$  represents the  $i^{th}$  optimization objective function, which typically includes accuracy or network scale. By identifying these Pareto optimal solutions, the algorithm gradually finds the optimal or near-optimal neural network architectures that satisfy multi-objective requirements.

We use the Hypervolume (HV) Indicator to quantify the quality of the Pareto front. This metric measures the multidimensional volume enclosed by the solution set in the objective space, which extends from the points in the solution set to a reference point. As the reference point, we select the worst point in the objective space, known as the Nadir Point. A larger HV value indicates better convergence and overall quality of the solution set. The formula for calculating the HV is as follows.

$$HV(S) = \text{Volume} \left( \bigcup_{x \in S} [f_1(x), f_1^{\text{ref}}] \times \dots \times [f_m(x), f_m^{\text{ref}}] \right) \quad (2)$$

$S$  is the solution set, which contains multiple solutions.  $f_i(x)$  is the value of the  $i^{th}$  objective function for solution  $x$ .  $f_i^{\text{ref}}$  is the reference point value for the  $i^{th}$  objective, typically chosen as the worst possible value for that objective. Volume represents the Hypervolume in multidimensional space, formed by the intervals between the solution points and the reference points.

### B. Upper Confidence Bound (UCB)

The UCB algorithm based on standard deviation is an effective strategy for solving the multi-armed bandit problem [2], aimed at balancing exploration and exploitation. The core concept of UCB revolves around directing the selection of actions by considering both the uncertainty of rewards associated with each action and the average rewards derived from all actions. The following formula shows how the UCB value for each action is calculated.

$$UCB = \bar{x}_j + c \cdot \sigma_j \quad (3)$$

Here,  $\bar{x}_j$  represents the average reward of action  $j$ ,  $\sigma_j$  represents the standard deviation of the reward for action  $j$ , and  $c$  is a positive parameter controlling the intensity of exploration. A larger  $c$  value tends to encourage more exploration, while a smaller  $c$  value emphasizes exploiting the known best action.

In each iteration, the algorithm returns the action with the highest UCB value. As experiments proceed, the average rewards and standard deviations for each action will gradually stabilize, and the algorithm's selections will increasingly lean towards the truly optimal action.

### C. Related Work

ENAS is proficient in managing extensive search spaces while utilizing minimal computational resources. The initial work of ENAS is widely acknowledged as the LargeEvo algorithm [4]. This algorithm utilized a genetic algorithm to determine the most effective CNN architecture. EvoOSNet [5] adopted a cell-based encoding method, enabling partial weight sharing and potentially reducing interference among candidate architectures during the evolutionary search process. Prenas [6] integrated a performance predictor with a limited number of evaluated architectures. Z. Lv *et al.* [7] defined and analyzed a binary classification problem to evaluate the performance of ENAS algorithms. J. Zou *et al.* [8] addressed limitations in search space design by segmenting the search into interconnected units to enhance network structure diversity while reducing computational costs.

<sup>1</sup>National Innovation Institute of Defense Technology, Academy of Military Sciences, Beijing, China sd9.xin@gmail.com, leiwang@nudt.edu.cn

<sup>2</sup>QiYuan Lab, Beijing, China chenrenzhil1989@qiyuanlab.com

<sup>3</sup>College of Computer, National University of Defence Technology, Changsha, China {xiaoxun520, liyuan22}@nudt.edu.cn

NAS for Spiking Neural Network (SNN) has significantly enhanced SNN designs, optimizing performance and efficiency across various applications. AutoSNN [9] analyzed the architectural impact on performance and spike generation, achieving optimal SNN configurations that outperform conventional hand-crafted designs. SNASNet [10] used diverse spike activation patterns without training, significantly improving performance on image recognition tasks with reduced timesteps. *Che et al.* [11] developed a spike-based differentiable hierarchical search that builds upon the DARTS framework established by *Liu et al.* [12]. Spikenas [13] is a framework used in autonomous mobile agents, significantly reducing search time and improving accuracy while adhering to specific memory constraints. LitE-SNN [14] is a method for designing lightweight and efficient SNN through spatial-temporal compressive network search and joint optimization.

Multi-objective ENAS leverages low-cost evaluation strategies to efficiently optimize neural network architectures, balancing performance and computational efficiency across various implementations. TF-MOENAS [15] used expressivity and trainability metrics without the need for training, thereby reducing computational costs. *Q. M. Phan et al.* [16] introduced a training-free Pareto local search that efficiently locates optimal solutions without the computational expense of training candidate architectures. E-TF-MOENAS [17] efficiently balanced network performance and complexity, utilizing low-cost proxy metrics for fast evaluation without full network training. GrMoNAS [18] leveraged coarse-to-fine granularity transformation and multi-objective optimization to achieve high diagnostic accuracy and efficiency within constrained computational resources. Although the aforementioned work has managed to balance multiple objectives in NAS, the challenge of huge search spaces has not been adequately addressed.

## II. RESULTS AND ANALYSIS

### A. The Pareto Fronts with Different $k$

Fig. 1 shows the Pareto fronts obtained under different  $k$  after 800 function evaluations.

### B. Pareto Solutions and Network Architecture

Table I presents the network structures corresponding to different Pareto solutions after 800 function evaluations with  $k = 1$ .

## REFERENCES

- [1] Giagkiozis I, Fleming PJ. Pareto front estimation for decision making. *Evolutionary computation*. 2014 Dec 1;22(4):651-78.
- [2] Kuleshov V, Precup D. Algorithms for multi-armed bandit problems. *arXiv preprint arXiv:1402.6028*. 2014 Feb 25.
- [3] Tian S, Qu L, Wang L, Hu K, Li N, Xu W. A neural architecture search based framework for liquid state machine design. *Neurocomputing*. 2021 Jul 5;443:174-82.
- [4] REAL, Esteban, et al. Large-scale evolution of image classifiers. In: *International conference on machine learning*. PMLR, 2017. p. 2902-2911.
- [5] ZHANG, Haoyu; JIN, Yaochu; HAO, Kuangrong. Evolutionary search for complete neural network architectures with partial weight sharing. *IEEE transactions on evolutionary computation*, 2022, 26.5: 1072-1086.
- [6] PENG, Yameng, et al. Pre-nas: Evolutionary neural architecture search with predictor. *IEEE Transactions on Evolutionary Computation*, 2022, 27.1: 26-36.
- [7] LV, Zeqiong; QIAN, Chao; SUN, Yanan. A First Step Towards Runtime Analysis of Evolutionary Neural Architecture Search. *arXiv preprint arXiv:2401.11712*, 2024.
- [8] ZOU, Juan, et al. Multiple Population Alternate Evolution Neural Architecture Search. *arXiv preprint arXiv:2403.07035*, 2024.
- [9] NA, Byunggook, et al. Autosnn: Towards energy-efficient spiking neural networks. In: *International Conference on Machine Learning*. PMLR, 2022. p. 16253-16269.
- [10] KIM, Youngeun, et al. Neural architecture search for spiking neural networks. In: *European Conference on Computer Vision*. Cham: Springer Nature Switzerland, 2022. p. 36-56.
- [11] CHE, Kaiwei, et al. Differentiable hierarchical and surrogate gradient search for spiking neural networks. *Advances in Neural Information Processing Systems*, 2022, 35: 24975-24990.
- [12] LIU, Hanxiao; SIMONYAN, Karen; YANG, Yiming. Darts: Differentiable architecture search. *arXiv preprint arXiv:1806.09055*, 2018.
- [13] PUTRA, Rachmad Vidya Wicaksana; SHAFIQUE, Muhammad. Spike-NAS: A Fast Memory-Aware Neural Architecture Search Framework for Spiking Neural Network Systems. *arXiv preprint arXiv:2402.11322*, 2024.
- [14] LIU, Qianhui, et al. LitE-SNN: Designing Lightweight and Efficient Spiking Neural Network through Spatial-Temporal Compressive Network Search and Joint Optimization. *arXiv preprint arXiv:2401.14652*, 2024.
- [15] DO, Tu; LUONG, Ngoc Hoang. Training-free multi-objective evolutionary neural architecture search via neural tangent kernel and number of linear regions. In: *Neural Information Processing: 28th International Conference, ICONIP 2021, Sanur, Bali, Indonesia, December 8–12, 2021, Proceedings, Part II* 28. Springer International Publishing, 2021. p. 335-347.
- [16] PHAN, Quan Minh; LUONG, Ngoc Hoang. Enhancing multi-objective evolutionary neural architecture search with training-free Pareto local search. *Applied Intelligence*, 2023, 53.8: 8654-8672.
- [17] LUONG, Ngoc Hoang, et al. Lightweight multi-objective evolutionary neural architecture search with low-cost proxy metrics. *Information Sciences*, 2024, 655: 119856.
- [18] LIU, Xin, et al. GrMoNAS: A granularity-based multi-objective NAS framework for efficient medical diagnosis. *Computers in Biology and Medicine*, 2024, 108118.

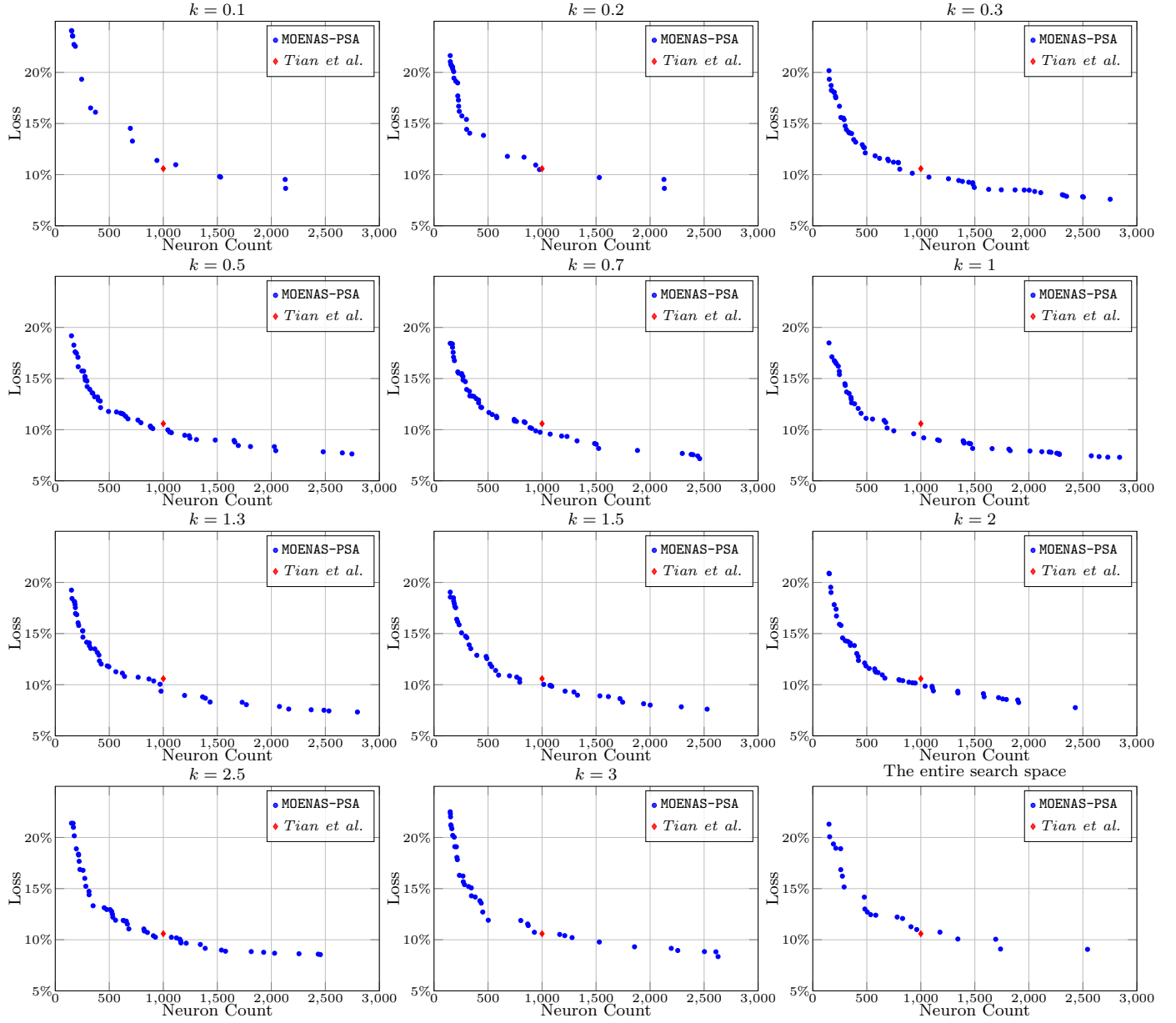


Fig. 1. The Pareto fronts obtained under different  $k$  after 800 function evaluations, including the unreduced search space.

TABLE I

THE NETWORK STRUCTURES CORRESPONDING TO DIFFERENT PARETO SOLUTIONS AFTER 800 FUNCTION EVALUATIONS WITH  $k = 1$ . ALL LIQUID STATE MACHINE MODELS ARE SINGLE-LAYER WITH THREE RESERVOIRS, WITH EACH ROW REPRESENTING THE PARAMETERS OF ONE RESERVOIR.

				Network Architecture					
		Loss	Neuron Count	$N$	Ratio	$P_{E \rightarrow E}$	$P_{E \rightarrow I}$	$P_{I \rightarrow E}$	$P_{I \rightarrow I}$
MOENAS-PSA	<i>Tian et al.</i> [3]	10.6%	1000	75	0.9	0.5	0.5	0.5	0.1
				505	0.8	0.4	0.3	0.4	0.0
				420	0.8	0.2	0.4	0.3	0.0
	Extreme Points	$N_E$	18.5%	<b>150</b>	50	0.89	0.0015	0.83	0.67
					50	0.81	0.0023	0.35	0.35
					50	0.90	0.0004	0.65	0.89
		$L_E$	7.3%	2840	924	0.88	0.0134	0.76	0.54
					991	0.78	0.0006	0.38	0.37
					925	0.90	0.0164	0.61	0.71
	Trade-off Points	$L_T$	9.2%	1027	419	0.88	0.060	0.84	0.54
					319	0.78	0.032	0.39	0.37
					289	0.90	0.002	0.61	0.77
		$N_T$	10.7%	675	51	0.89	0.00517	0.83	0.69
					336	0.81	0.00004	0.35	0.35
					288	0.90	0.00130	0.65	0.86
	Knee Point	$K$	9.9%	750	183	0.88	0.17	0.84	0.54
					331	0.78	0.03	0.42	0.37
					236	0.83	0.04	0.31	0.77